Received: December 20, 2019 | Accepted: January 16, 2020 | Web Released: January 22, 2020 CL-190930

Low-temperature Conversion of Carbon Dioxide to Methane in an Electric Field

Kensei Yamada, Shuhei Ogo, Ryota Yamano, Takuma Higo, and Yasushi Sekine*
Applied Chemistry, Waseda University, 3-4-1 Okubo, Shinjuku, Tokyo 169-8555, Japan

E-mail: ysekine@waseda.jp

CO_2 methanation was conducted at low temperatures with an electric field. Results show that 5 wt%Ru/CeO_2 catalyst exhibited high and stable catalytic activity for CO_2 methanation with the electric field. The kinetic investigations and *in-situ* DRIFTS measurements revealed that Ru/CeO_2 catalyst promoted CO_2 methanation and Ru at the Ru–CeO_2 interface (low-coordinated Ru sites) contributes to the reverse water gas shift reaction at low temperatures in the electric field.

Keywords: Carbon dioxide | Electric field | Methane

Conversion of CO_2 to valuable chemicals such as CO, CH_4, and CH_3OH, has drawn great attention for use in supporting carbon capture and utilization (CCU).[1–4] One established CO_2 conversion process is CO_2 methanation (eq (1)), known as the Sabatier reaction.

$$CO_2 + 4H_2 \rightarrow CH_4 + 2H_2O \quad \Delta H^\circ_{298} = -164.9\,\mathrm{kJ\,mol^{-1}} \quad (1)$$

Methane (CH_4) can be used not only as fuel but also as a hydrogen carrier via transportation in existing infrastructure for town gas.[5,6] Especially in Germany, some plants have already been launched based on the concept of "Power to Gas".[7,8]

Moreover, CO_2 methanation is operated industrially using Ni-based and Ru-based catalysts at temperatures of 523–673 K with pressures of 1–300 bar.[9–12] Considering the thermodynamic equilibrium, operation at low temperatures is favorable to improve CO_2 conversion and CH_4 selectivity because reverse reaction (steam reforming of CH_4) and side reaction (reverse water gas shift: RWGS, eq (2)) are suppressed at low temperatures.

$$CO_2 + H_2 \rightarrow CO + H_2O \quad \Delta H^\circ_{298} = 41.2\,\mathrm{kJ\,mol^{-1}} \quad (2)$$

However, the dissociation of CO_2 has a high activation barrier because of the high thermodynamic stability of CO_2.[13] Recently, to decrease the reaction temperature, unconventional reaction systems such as electrocatalysis and photocatalysis have been applied intensively to CO_2 methanation.[14–17]

Earlier, we demonstrated that CO_2 is activated even at low temperatures by application of a direct current electric field (EF) to heterogeneous catalyst supported on a semiconductor for some reactions: dry reforming of methane,[18–22] RWGS,[23] and oxidative coupling of methane using carbon dioxide.[24] Regarding dry reforming of methane, Ni-supported on La-ZrO_2 catalyst exhibited high catalytic activity, even at 423 K in EF. Investigations of isotope effects and *in-situ* DRIFTS measurements suggest that proton conduction on the catalyst surface occurs in EF and that it contributes to CO_2 activation.

This work revealed that Ru catalyst supported on CeO_2 showed good activity for CO_2 methanation, even at low temperatures in an EF. We studied the role of EF in the reaction by comparison with conventional (not imposing an EF) catalytic reaction. We demonstrated that imposing an EF activates CO_2 in a non-conventional catalytic mechanism.

Ru-supported on CeO_2 catalysts were prepared using an impregnation method. First, Ru precursor ($Ru(acac)_3$) was dissolved in acetone followed by adding CeO_2 powder (JRC-CEO-1). After stirring at room temperature for 2 h, the suspension was heated to 423 K for the evaporation of solvent. The obtained powder was dried at 393 K overnight and was heated to 723 K for 2 h under a reducing atmosphere (50%H_2 flow). The prepared catalyst was sieved into 355–500 µm particles. Activity tests were performed in a fixed bed flow-type reactor (quartz tubes, 6 mm i.d., 8 mm o.d.). Two stainless steel electrodes (2 mm o.d.) were inserted contiguously to the top and bottom of the catalyst bed to impose an electric field. The catalyst (80 or 100 mg) was reduced at 723 K in H_2:Ar = 1:3 (100 SCCM total flow rate) before the reaction. Direct current of 5.0 mA was imposed to the catalyst bed using a DC power supply. The applied voltage profile, as measured using an oscilloscope (TDS 3052B; Tektronix Inc.), was stable (150 V), not forming discharge/plasma during the reaction. The reactant feed gases were carbon dioxide, hydrogen, and argon in the ratio of CO_2:H_2:Ar = 1:4:5 (100 SCCM total flow rate for the screening tests; 200 SCCM for the other tests). In the activity tests for the evaluation of partial pressure effects for CO_2 and H_2, the reactant feed gases in various H_2/CO_2 ratios were arranged to the total flow rate of 200 SCCM by diluted Ar. Gaseous products including CO, CH_4, and CO_2 were analyzed using GC-FID (GC-14B; Shimadzu Corp.) equipped with a Porapak N packed column and a methanizer (Ru/Al_2O_3 catalyst). A cold trap was placed at the exit of the reactor to condense water that formed. The respective calculation formulae for CO_2 conversion, CH_4 selectivity, and CO_2 consumption rate are shown below (eq 3–5).

$$CO_2\ \text{conversion}\ (\%) = (F_{\mathrm{CO,out}} + F_{\mathrm{CH4,out}})/F_{\mathrm{CO2,in}} \times 100 \quad (3)$$

$$CH_4\ \text{selectivity}\ (\%) = F_{\mathrm{CH4,out}}/(F_{\mathrm{CO,out}} + F_{\mathrm{CH4,out}}) \times 100 \quad (4)$$

$$CO_2\ \text{consumption rate},\ r = F_{\mathrm{CO,out}} + F_{\mathrm{CH4,out}} \quad (5)$$

In these equations, F_{out} denotes the product formation rate; F_{in} denotes the reactant supply rate. Calculated carbon balances were almost 100%. Only CO and CH_4 were detected as carbon-containing products, indicating the carbon deposition as negligible.

In-situ DRIFTS measurements were conducted using a FT-IR spectrophotometer (FT/IR-6200; Jasco Corp.) equipped with an MCT-M detector and a ZnSe window. The sieved catalyst (150 mg) was charged in a DRIFTS cell made of Teflon with two pinholes to insert electrodes, as described in an earlier report.[25] Before measurement, the catalyst was reduced at 573 K in H_2 flow for 120 min and was then purged in Ar flow for 30 min. The background spectra were recorded under Ar gas (15 SCCM) at 343 K with EF or at 493 K without EF. All spectra were recorded with 4 cm^{-1} resolution and 20 scans. The applied current was 5.0 mA. The response voltage was about 0.20 kV.

Table 1 presents results of activity tests conducted over various metal catalysts supported on CeO_2 in an EF at 343 K furnace temperature. The catalyst bed temperature was measured

Table 1. Results of activity tests over various metal-supported catalysts in an electric field

catalysts	Temp / K	Current / mA	Voltage / kV	Power / W	CO_2 Conv. / %	CH_4 Sel. / %	CO sel. / %
5wt%Ru/CeO_2	416	5	0.17	0.84	17.4	96.4	3.6
0.5wt%Ru/CeO_2	405	5	0.17	0.83	7.5	26.9	73.1
5wt%Ni/CeO_2	428	5	0.23	1.13	11.2	63.6	36.4
5wt%Co/CeO_2	406	5	0.18	0.90	5.2	9.1	90.9
5wt%Cu/CeO_2	396	5	0.16	0.79	3.7	0.0	100.0
5wt%Fe/CeO_2	394	5	0.16	0.80	4.1	0.0	100.0

CO_2:H_2:Ar = 1:4:5; 100 SCCM total flow rate; 5.0 mA input current; 100 mg catalyst weight; 343 K furnace temperature

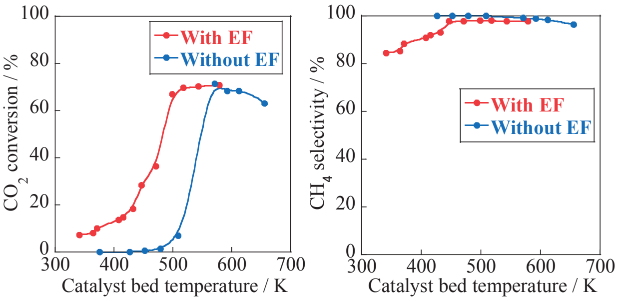

Figure 1. Temperature dependence of catalytic activity and selectivity with and without the electric field over Ru/CeO_2 catalyst (CO_2:H_2:Ar = 1:4:5; 200 SCCM total flow rate; 5.0 mA input current; 100 mg catalyst weight).

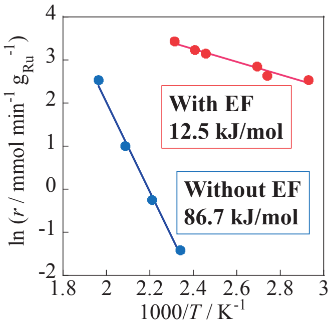

Figure 2. Arrhenius plots for CO_2 hydrogenation reaction over Ru/CeO_2 catalyst with and without the electric field.

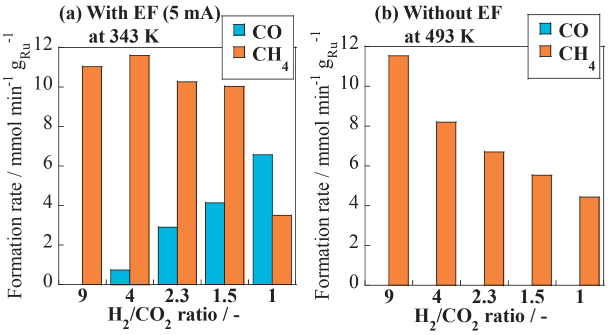

Figure 3. CH_4 and CO formation rates over Ru/CeO_2 catalyst under various H_2/CO_2 ratios (a) with EF at 343 K or (b) without EF at 493 K (CO_2:H_2:Ar = (1–5):(9–5):10; 200 SCCM total flow rate; 100 mg catalyst weight).

directly using a thermocouple attached to the bottom of the catalyst bed to consider the Joule heat and reaction heat. Results show that CO was formed over all the tested metal catalysts, whereas CH_4 was formed over Ru, Ni or Co supported catalyst. Especially, 5 wt%Ru/CeO_2 catalyst showed the highest CO_2 conversion and CH_4 selectivity (17.4% and 96.4%, respectively) among the tested metal catalysts. 0.5 wt%Ru/CeO_2 catalyst showed much lower CH_4 selectivity than 5 wt% Ru/CeO_2 did. Table S1 (in Supporting information) shows the relationship between Ru loading and Ru particle size. Actually, CH_4 selectivity is known to depend strongly on the Ru particle size.[26,27] Small clusters or isolated species of Ru are favorable to form CO with high selectivity. Therefore, 5 wt%Ru/CeO_2 (denoted as Ru/CeO_2) is a suitable catalyst for CO_2 methanation in EF.

To elucidate the effects of EF on the activity of Ru/CeO_2 catalyst for CO_2 methanation, catalytic activity tests were conducted with and without EF at various temperatures (Figure 1). The CO_2 methanation proceeded at 340 K with an EF, whereas it proceeded at temperatures higher than 430 K without an EF. The CH_4 selectivity increased to approximately 98% from 340 to 445 K with an EF. Then it reached a plateau at higher temperatures. However, without an EF, the CH_4 selectivity was almost 100% below 570 K and CO was detected over 570 K. Figure 2 shows Arrhenius plots of CO_2 consumption rates with and without an EF under kinetic conditions. The apparent activation energy E_a with an EF (12.5 kJ/mol) was much lower than that without an EF (86.7 kJ/mol). These results indicate that CO_2 methanation is promoted at low temperature by imposing an EF *via* a different mechanism from that of the conventional catalytic reaction without an EF. In addition, the catalytic stability of Ru/CeO_2 with or without an EF was evaluated at almost identical initial CO_2 conversion (Figure S1). The activity with an EF was stable until at least 90 min whereas that without an EF decreased gradually. One can infer that reaction intermediates derived from CO_2 strongly adsorb on the Ru surface and that they inhibit the reaction without an EF.

Next, we investigated the reaction pathway in CO_2 methanation with EF. Figure S2 shows the effects of the contact time (W/F) on catalytic activity over Ru/CeO_2 with an EF. As the contact time increased, the CH_4 selectivity increased. This finding demonstrates that CO is an intermediate in CO_2 methanation with an EF.

Then, the influence of H_2/CO_2 ratio of the reactant gas on CH_4 and CO formation rates was investigated under kinetic conditions (Figure 3). The CH_4 formation rate with an EF reached a maximum under a stoichiometric ratio for CO_2 methanation (H_2/CO_2 = 4). Thereafter, it decreased as the H_2/CO_2 ratio decreased. Moreover, the CO formation rate increased concomitantly as the H_2/CO_2 ratio decreased. However, in the reaction without an EF, CO was not detected in any H_2/CO_2 ratio, even though the CH_4 formation rate decreased monotonically with decreasing H_2/CO_2 ratio. These results indicated that the H_2/CO_2 ratio affects CH_4 selectivity with an EF, and it affects CO_2 conversion rate without EF.

Figure 4 presents the effects of the partial pressures of CO_2 and H_2 on the CO_2 consumption rate with and without EF. The CO_2 consumption rate denoted as r is assumed as the following equation (eq 6) using CO_2 and H_2 partial pressures.

$$r = kP_{CO2}{}^{\alpha}P_{H2}{}^{\beta} \quad (6)$$

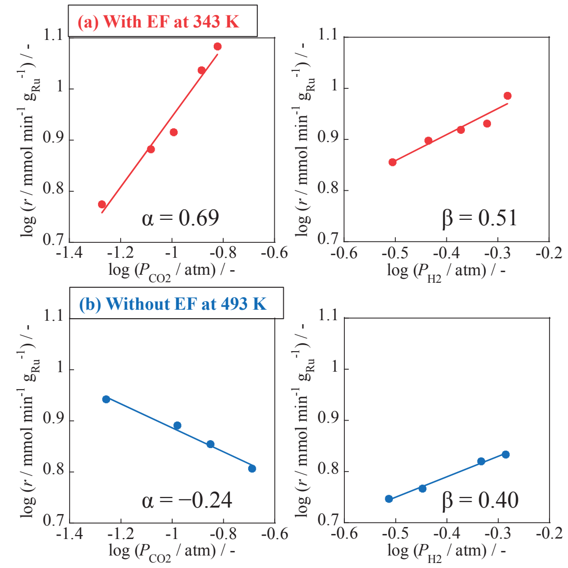

Figure 4. Effects of partial pressures of CO_2 and H_2 on the CO_2 consumption rate over Ru/CeO_2 catalyst (a) with EF at 343 K and (b) without EF at 493 K (80 mg catalyst weight).

The reaction orders of the CO_2 and H_2 partial pressures for the CO_2 consumption rate without an EF were, respectively, −0.24 and 0.40. According to earlier reports for Ru/CeO_2 catalyst, the negative order of CO_2 partial pressure is attributable to strong CO adsorption on the Ru surface.[28,29] In contrast, the CO_2 consumption rate with an EF was correlated positively with the CO_2 partial pressure. Therefore, the hindrance of adsorbed CO is eliminated by imposing an EF. Additionally, the reaction order of CO_2 partial pressure (0.69) was larger than that of H_2 partial pressure (0.51) with EF, which suggests that the CO_2 consumption rate depends on the RWGS reaction rate. This demonstrates that CO_2 is converted to CO *via* RWGS reaction, and then CO is hydrogenated to CH_4. It is inferred that CO methanation proceeds faster than RWGS reaction with EF, so high CH_4 selectivity is achieved over Ru/CeO_2.

To elucidate the reaction mechanism in CO_2 methanation with an EF further, *in-situ* DRIFTS measurements were conducted. Figure S3 shows the DRIFT spectra measured during the reaction ($H_2/CO_2 = 4$) with and without an EF. The broad band assigned to carbonyl species adsorbed onto the Ru particle surface was observed around 2070–1870 cm^{-1}. It can be divided to three peaks (Table S2).[28,30] To investigate the H_2/CO_2 ratio effects on adsorbed species over Ru/CeO_2 with or without an EF, DRIFT spectra were recorded after 20 min of the reaction with or without an EF under different H_2/CO_2 ratios (Figure 5). Without an EF, no significant difference was found by changing the H_2/CO_2 ratio. However, with an EF, the intensities of the bands assigned to the adsorbed CO on low-coordinated Ru sites (1975 cm^{-1}) and gaseous CO (2100–2200 cm^{-1}) increased as the H_2/CO_2 ratio decreased, which suggests that the low-coordinated Ru site is active for RWGS reaction with an EF. Based on the positive order of CO_2 partial pressure, it is also inferred that CO adsorption on the Ru surface is weakened in an EF so that the low-coordinated Ru site is active for CO_2 conversion *via* RWGS reaction. CO desorption from Ru could bring low CH_4 selectivity. Hence the rate of CO methanation in EF is also important. CO methanation is known to proceed above 473 K over Ru/TiO_2 catalyst in the conventional catalytic system (without an EF).[31] With an EF, Ru/CeO_2 catalyst exhibited high CH_4 selectivity (96.4%) at 416 K. That indicates an EF also accelerates CO methanation.

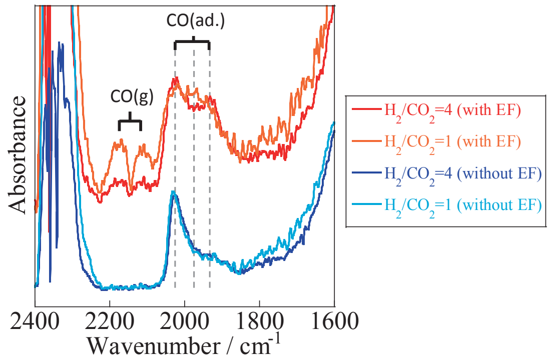

Figure 5. *In-situ* DRIFT spectra after reaction under different H_2/CO_2 ratios (1 or 4) over Ru/CeO_2 catalyst with EF (5 mA) at 343 K or without EF at 493 K (CO_2:H_2:Ar = 2:8:5 or 5:5:5; 15 SCCM total flow rate).

To ascertain the active CO species on the Ru surface in the reaction, the spectra were recorded during H_2 flow after the reaction gas exposure under $H_2/CO_2 = 1$ (Figure 6). In the reaction without EF, only CO adsorbed onto highly coordinated Ru

(a) With EF (5 mA) at 343 K

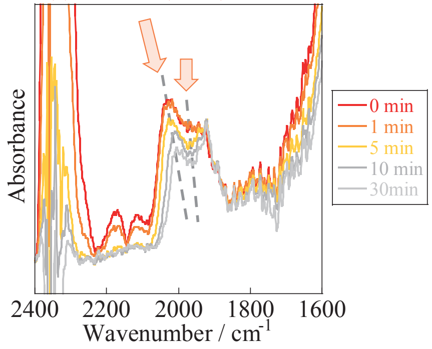

(b) Without EF at 493 K

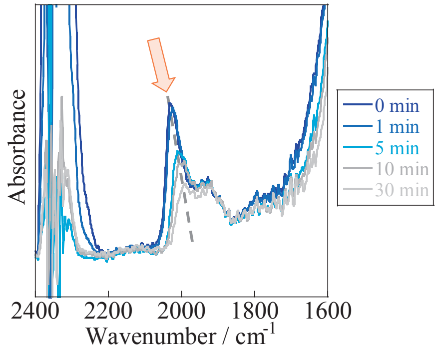

Figure 6. *In-situ* DRIFT spectra during H_2 flow after the reaction under $H_2/CO_2 = 1$ over Ru/CeO_2 catalyst (a) with EF (5 mA) at 343 K and (b) without EF at 493 K (CO_2:H_2:Ar = 5:5:5 or 0:5:10; 15 SCCM total flow rate).

sites (2025 cm^{-1}) decreased rapidly. Reportedly, CO_2 methanation is a structure-sensitive reaction because the turnover frequency increases concomitantly with increasing Ru particle size.[28,32] This result indicates that low-coordinated Ru sites, i.e. small clusters of Ru or the Ru at Ru–CeO_2 interface, are less active for CO_2 methanation. However, two CO species adsorbed onto high-coordinated and low-coordinated Ru sites (2025 and 1975 cm^{-1}) were converted with an EF, which indicates that these adsorbed species are reactive for the reaction in an EF. Therefore, in CO_2 methanation with an EF, not only large particles of Ru (high-coordinated Ru sites) but also small clusters of Ru and Ru at the Ru–CeO_2 interface (low-coordinated Ru sites) contribute to the reaction and thereby achieve high activity at low temperatures.

In summary, CO_2 methanation was conducted by imposing an electric field. Screening tests revealed that 5 wt %Ru/CeO_2 catalyst is a suitable catalyst for CO_2 methanation with the electric field. The electric field promoted the reaction over Ru/CeO_2 catalyst even at low temperatures such as 340 K *via* a non-conventional catalytic mechanism. The kinetic investigations and *in-situ* DRIFTS measurements revealed that CO_2 methanation with the electric field proceeds not only over highly coordinated Ru sites but also over low-coordinated Ru sites by virtue of the promotion of RWGS reaction at low-coordinated Ru sites. Ru/CeO_2 catalyst exhibits high and stable activity for CO_2 methanation without the hindrance of CO adsorbed onto the Ru particle surface.

Supporting Information is available on https://doi.org/10.1246/cl.190930.

References

1 W. Wang, S. Wang, X. Ma, J. Gong, *Chem. Soc. Rev.* **2011**, *40*, 3703.
2 M. Mikkelsen, M. Jørgensen, F. C. Krebs, *Energy Environ. Sci.* **2010**, *3*, 43.
3 A. M. Appel, J. E. Bercaw, A. B. Bocarsly, H. Dobbek, D. L. DuBois, M. Dupuis, J. G. Ferry, E. Fujita, R. Hille, P. J. A. Kenis, C. A. Kerfeld, R. H. Morris, C. H. F. Peden, A. R. Portis, S. W. Ragsdale, T. B. Rauchfuss, J. N. H. Reek, L. C. Seefeldt, R. K. Thauer, G. L. Waldrop, *Chem. Rev.* **2013**, *113*, 6621.
4 I. Dimitriou, P. García-Gutiérrez, R. H. Elder, R. M. Cuéllar-Franca, A. Azapagic, R. W. K. Allen, *Energy Environ. Sci.* **2015**, *8*, 1775.
5 P. T. Aakko-Saksa, C. Cook, J. Kiviaho, T. Repo, *J. Power Sources* **2018**, *396*, 803.
6 S. Tada, T. Shimizu, H. Kameyama, T. Haneda, R. Kikuchi, *Int. J. Hydrogen Energy* **2012**, *37*, 5527.
7 M. Götz, J. Lefebvre, F. Mörs, A. M. Koch, F. Graf, S. Bajohr, R. Reimert, T. Kolb, *Renew. Energy* **2016**, *85*, 1371.
8 G. Gahleitner, *Int. J. Hydrogen Energy* **2013**, *38*, 2039.
9 C. V. Miguel, A. Mendes, L. M. Madeira, *J. CO_2 Util.* **2018**, *25*, 128.
10 S. Schiebahn, T. Grube, M. Robinius, V. Tietze, B. Kumar, D. Stolten, *Int. J. Hydrogen Energy* **2015**, *40*, 4285.
11 P. Frontera, A. Macario, M. Ferraro, P. Antonucci, *Catalysts* **2017**, *7*, 59.
12 S. Rönsch, J. Schneider, S. Matthischke, M. Schlüter, M. Götz, J. Lefebvre, P. Prabhakaran, S. Bajohr, *Fuel* **2016**, *166*, 276.
13 J. Ko, B.-K. Kim, J. W. Han, *J. Phys. Chem. C* **2016**, *120*, 3438.
14 R. Dębek, F. Azzolina-Jury, A. Travert, F. Maugé, F. Thibault-Starzyk, *Catal. Today* **2019**, *337*, 182.
15 C. J. Lee, D. H. Lee, T. Kim, *Catal. Today* **2017**, *293–294*, 97.
16 R. Dębek, F. Azzolina-Jury, A. Travert, F. Maugé, *Renewable Sustainable Energy Rev.* **2019**, *116*, 109427.
17 G. R. Dey, A. D. Belapurkar, K. Kishore, *J. Photochem. Photobiol., A* **2004**, *163*, 503.
18 T. Yabe, Y. Sekine, *Fuel Process. Technol.* **2018**, *181*, 187.
19 T. Yabe, K. Mitarai, K. Oshima, S. Ogo, Y. Sekine, *Fuel Process. Technol.* **2017**, *158*, 96.
20 T. Yabe, K. Yamada, K. Murakami, K. Toko, K. Ito, T. Higo, S. Ogo, Y. Sekine, *ACS Sustainable Chem. Eng.* **2019**, *7*, 5690.
21 T. Oguri, K. Sugiura, T. Yabe, S. Ogo, Y. Sekine, *J. Jpn. Pet. Inst.* **2017**, *60*, 232.
22 T. Yabe, K. Yamada, T. Oguri, T. Higo, S. Ogo, Y. Sekine, *ACS Catal.* **2018**, *8*, 11470.
23 K. Oshima, T. Shinagawa, Y. Nogami, R. Manabe, S. Ogo, Y. Sekine, *Catal. Today* **2014**, *232*, 27.
24 T. Yabe, Y. Kamite, K. Sugiura, S. Ogo, Y. Sekine, *J. CO_2 Util.* **2017**, *20*, 156.
25 S. Okada, R. Manabe, R. Inagaki, S. Ogo, Y. Sekine, *Catal. Today* **2018**, *307*, 272.
26 A. Aitbekova, L. Wu, C. J. Wrasman, A. Boubnov, A. S. Hoffman, E. D. Goodman, S. R. Bare, M. Cargnello, *J. Am. Chem. Soc.* **2018**, *140*, 13736.
27 J. H. Kwak, L. Kovarik, J. Szanyi, *ACS Catal.* **2013**, *3*, 2449.
28 Y. Guo, S. Mei, K. Yuan, D.-J. Wang, H.-C. Liu, C.-H. Yan, Y.-W. Zhang, *ACS Catal.* **2018**, *8*, 6203.
29 J. A. H. Dreyer, P. Li, L. Zhang, G. K. Beh, R. Zhang, P. H.-L. Sit, W. Y. Teoh, *Appl. Catal., B* **2017**, *219*, 715.
30 S. Y. Chin, C. T. Williams, M. D. Amiridis, *J. Phys. Chem. B* **2006**, *110*, 871.
31 P. Panagiotopoulou, D. I. Kodarides, X. E. Verykios, *J. Phys. Chem. C* **2011**, *115*, 1220.
32 Z. Kowalczyk, K. Stołecki, W. Raróg-Pilecka, E. Miśkiewicz, E. Wilczkowska, Z. Karpiński, *Appl. Catal., A* **2008**, *342*, 35.